Author(s): PHENIX Collaboration

Title: Measurement of Direct-Photon Cross Section and Double-Helicity Asymmetry at $\sqrt{s}$ = 510 GeV in →p+→p Collisions

Year: 2023

Version: Published version

Please cite the original version:

PHENIX Collaboration. (2023). Measurement of Direct-Photon Cross Section and Double-Helicity Asymmetry at $\sqrt{s}$ = 510 GeV in →p+→p Collisions. Physical Review Letters, 130, Article 251901. https://doi.org/10.1103/PhysRevLett.130.251901

Measurement of Direct-Photon Cross Section and Double-Helicity Asymmetry at $\sqrt{s}=510$ GeV in $\vec{p}+\vec{p}$ Collisions

N. J. Abdulameer,[14] U. Acharya,[19] A. Adare,[11] C. Aidala,[42] N. N. Ajitanand,[61,*] Y. Akiba,[56,57,†] R. Akimoto,[10] M. Alfred,[22]
N. Apadula,[27,62] Y. Aramaki,[56] H. Asano,[34,56] E. T. Atomssa,[62] T. C. Awes,[52] B. Azmoun,[7] V. Babintsev,[23] M. Bai,[6]
N. S. Bandara,[40] B. Bannier,[62] K. N. Barish,[8] S. Bathe,[5,57] A. Bazilevsky,[7] M. Beaumier,[8] S. Beckman,[11] R. Belmont,[11,50]
A. Berdnikov,[59] Y. Berdnikov,[59] L. Bichon,[67] D. Black,[8] B. Blankenship,[67] J. S. Bok,[49] V. Borisov,[59] K. Boyle,[57]
M. L. Brooks,[37] J. Bryslawskyj,[5,8] H. Buesching,[7] V. Bumazhnov,[23] S. Campbell,[12,27] V. Canoa Roman,[62] C.-H. Chen,[57]
M. Chiu,[7] C. Y. Chi,[12] I. J. Choi,[24] J. B. Choi,[29,*] T. Chujo,[66] Z. Citron,[68] M. Connors,[19] R. Corliss,[62] Y. Corrales Morales,[37]
M. Csanád,[15] T. Csörgő,[41,69] A. Datta,[48] M. S. Daugherity,[1] G. David,[7,62] C. T. Dean,[37] K. DeBlasio,[48] K. Dehmelt,[62]
A. Denisov,[23] A. Deshpande,[57,62] E. J. Desmond,[7] L. Ding,[27] A. Dion,[62] V. Doomra,[62] J. H. Do,[70] A. Drees,[62] K. A. Drees,[6]
J. M. Durham,[37] A. Durum,[23] H. En'yo,[56] A. Enokizono,[56,58] R. Esha,[62] B. Fadem,[44] W. Fan,[62] N. Feege,[62] D. E. Fields,[48]
M. Finger, Jr.,[9] M. Finger,[9] D. Firak,[14,62] D. Fitzgerald,[42] S. L. Fokin,[33] J. E. Frantz,[51] A. Franz,[7] A. D. Frawley,[18]
P. Gallus,[13] C. Gal,[62] P. Garg,[3,62] H. Ge,[62] M. Giles,[62] F. Giordano,[24] A. Glenn,[36] Y. Goto,[56,57] N. Grau,[2] S. V. Greene,[67]
M. Grosse Perdekamp,[24] T. Gunji,[10] H. Guragain,[19] Y. Gu,[61] T. Hachiya,[46,56,57] J. S. Haggerty,[7] K. I. Hahn,[16] H. Hamagaki,[10]
J. Hanks,[62] S. Y. Han,[16,32] M. Harvey,[64] S. Hasegawa,[28] T. K. Hemmick,[62] X. He,[19] J. C. Hill,[27] A. Hodges,[19,24] R. S. Hollis,[8]
K. Homma,[21] B. Hong,[32] T. Hoshino,[21] J. Huang,[7,37] Y. Ikeda,[56] K. Imai,[28] Y. Imazu,[56] M. Inaba,[66] A. Iordanova,[8]
D. Isenhower,[1] D. Ivanishchev,[54] B. V. Jacak,[62] S. J. Jeon,[45] M. Jezghani,[19] X. Jiang,[37] Z. Ji,[62] B. M. Johnson,[7,19] E. Joo,[32]
K. S. Joo,[45] D. Jouan,[53] D. S. Jumper,[24] J. H. Kang,[70] J. S. Kang,[20] D. Kawall,[40] A. V. Kazantsev,[33] J. A. Key,[48]
V. Khachatryan,[62] A. Khanzadeev,[54] A. Khatiwada,[37] K. Kihara,[66] C. Kim,[32] D. H. Kim,[16] D. J. Kim,[30] E.-J. Kim,[29]
H.-J. Kim,[70] M. Kim,[60] T. Kim,[16] Y. K. Kim,[20] D. Kincses,[15] A. Kingan,[62] E. Kistenev,[7] J. Klatsky,[18] D. Kleinjan,[8]
P. Kline,[62] T. Koblesky,[11] M. Kofarago,[15,69] J. Koster,[57] D. Kotov,[54,59] L. Kovacs,[15] B. Kurgyis,[15] K. Kurita,[58]
M. Kurosawa,[56,57] Y. Kwon,[70] J. G. Lajoie,[27] D. Larionova,[59] A. Lebedev,[27] K. B. Lee,[37] S. H. Lee,[27,42,62] M. J. Leitch,[37]
M. Leitgab,[24] N. A. Lewis,[42] S. H. Lim,[55,70] M. X. Liu,[37] X. Li,[37] D. A. Loomis,[42] D. Lynch,[7] S. Lökös,[15] T. Majoros,[14]
Y. I. Makdisi,[6] M. Makek,[68,71] A. Manion,[62] V. I. Manko,[33] E. Mannel,[7] M. McCumber,[37] P. L. McGaughey,[37]
D. McGlinchey,[11,37] C. McKinney,[24] A. Meles,[49] M. Mendoza,[8] B. Meredith,[12] Y. Miake,[66] A. C. Mignerey,[39] A. J. Miller,[1]
A. Milov,[68] D. K. Mishra,[4] J. T. Mitchell,[7] M. Mitrankova,[59] Iu. Mitrankov,[59] S. Miyasaka,[56,65] S. Mizuno,[56,66]
M. M. Mondal,[62] P. Montuenga,[24] T. Moon,[32,70] D. P. Morrison,[7] T. V. Moukhanova,[33] A. Muhammad,[43] B. Mulilo,[32,56,72]
T. Murakami,[34,56] J. Murata,[56,58] A. Mwai,[61] S. Nagamiya,[31,56] J. L. Nagle,[11] M. I. Nagy,[15] I. Nakagawa,[56,57]
H. Nakagomi,[56,66] K. Nakano,[56,65] C. Nattrass,[63] S. Nelson,[17] P. K. Netrakanti,[4] M. Nihashi,[21,56] T. Niida,[66] R. Nouicer,[7,57]
N. Novitzky,[30,62,66] G. Nukazuka,[56,57] A. S. Nyanin,[33] E. O'Brien,[7] C. A. Ogilvie,[27] J. Oh,[55] J. D. Orjuela Koop,[11]
M. Orosz,[14] J. D. Osborn,[42,52] A. Oskarsson,[38] K. Ozawa,[31,66] R. Pak,[7] V. Pantuev,[25] V. Papavassiliou,[49] J. S. Park,[60]
S. Park,[43,60,62] L. Patel,[19] M. Patel,[27] S. F. Pate,[49] J.-C. Peng,[24] W. Peng,[67] D. V. Perepelitsa,[7,11,12] G. D. N. Perera,[49]
D. Yu. Peressounko,[33] C. E. PerezLara,[62] J. Perry,[27] R. Petti,[7,62] C. Pinkenburg,[7] R. Pinson,[1] R. P. Pisani,[7] M. Potekhin,[7]
A. Pun,[51] M. L. Purschke,[7] P. V. Radzevich,[59] J. Rak,[30] N. Ramasubramanian,[62] I. Ravinovich,[68] K. F. Read,[52,63]
D. Reynolds,[61] V. Riabov,[47,54] Y. Riabov,[54,59] D. Richford,[5] N. Riveli,[51] D. Roach,[67] S. D. Rolnick,[8] M. Rosati,[27] Z. Rowan,[5]
J. G. Rubin,[42] J. Runchey,[27] N. Saito,[31] T. Sakaguchi,[7] H. Sako,[28] V. Samsonov,[47,54] M. Sarsour,[19] S. Sato,[28] S. Sawada,[31]
B. Schaefer,[67] B. K. Schmoll,[63] K. Sedgwick,[8] J. Seele,[57] R. Seidl,[56,57] A. Sen,[27,63] R. Seto,[8] P. Sett,[4] A. Sexton,[39]
D. Sharma,[62] I. Shein,[23] M. Shibata,[46] T.-A. Shibata,[56,65] K. Shigaki,[21] M. Shimomura,[27,46] Z. Shi,[37] P. Shukla,[4]
A. Sickles,[7,24] C. L. Silva,[37] D. Silvermyr,[38,52] B. K. Singh,[3] C. P. Singh,[3,*] V. Singh,[3] M. Slunečka,[9] K. L. Smith,[18]
R. A. Soltz,[36] W. E. Sondheim,[37] S. P. Sorensen,[63] I. V. Sourikova,[7] P. W. Stankus,[52] M. Stepanov,[40,*] S. P. Stoll,[7]
T. Sugitate,[21] A. Sukhanov,[7] T. Sumita,[56] J. Sun,[62] Z. Sun,[14] J. Sziklai,[69] R. Takahama,[46] A. Takahara,[10] A. Taketani,[56,57]
K. Tanida,[28,57,60] M. J. Tannenbaum,[7] S. Tarafdar,[67,68] A. Taranenko,[47,61] A. Timilsina,[27] T. Todoroki,[56,57,66] M. Tomášek,[13]
H. Torii,[10] M. Towell,[1] R. Towell,[1] R. S. Towell,[1] I. Tserruya,[68] Y. Ueda,[21] B. Ujvari,[14] H. W. van Hecke,[37] M. Vargyas,[15,69]
J. Velkovska,[67] M. Virius,[13] V. Vrba,[13,26] E. Vznuzdaev,[54] X. R. Wang,[49,57] Z. Wang,[5] D. Watanabe,[21] Y. Watanabe,[56,57]
Y. S. Watanabe,[10,31] F. Wei,[49] S. Whitaker,[27] S. Wolin,[24] C. P. Wong,[19,37] C. L. Woody,[7] M. Wysocki,[52] B. Xia,[51]
L. Xue,[19] S. Yalcin,[62] Y. L. Yamaguchi,[10,62] A. Yanovich,[23] I. Yoon,[60] I. Younus,[35] I. E. Yushmanov,[33] W. A. Zajc,[12]
A. Zelenski,[6] and L. Zou[8]

(PHENIX Collaboration)

[1]*Abilene Christian University, Abilene, Texas 79699, USA*
[2]*Department of Physics, Augustana University, Sioux Falls, South Dakota 57197, USA*
[3]*Department of Physics, Banaras Hindu University, Varanasi 221005, India*
[4]*Bhabha Atomic Research Centre, Bombay 400 085, India*
[5]*Baruch College, City University of New York, New York, New York 10010, USA*
[6]*Collider-Accelerator Department, Brookhaven National Laboratory, Upton, New York 11973-5000, USA*
[7]*Physics Department, Brookhaven National Laboratory, Upton, New York 11973-5000, USA*
[8]*University of California-Riverside, Riverside, California 92521, USA*
[9]*Charles University, Faculty of Mathematics and Physics, 180 00 Troja, Prague, Czech Republic*
[10]*Center for Nuclear Study, Graduate School of Science, University of Tokyo, 7-3-1 Hongo, Bunkyo, Tokyo 113-0033, Japan*
[11]*University of Colorado, Boulder, Colorado 80309, USA*
[12]*Columbia University, New York, New York 10027 and Nevis Laboratories, Irvington, New York 10533, USA*
[13]*Czech Technical University, Zikova 4, 166 36 Prague 6, Czech Republic*
[14]*Debrecen University, H-4010 Debrecen, Egyetem tér 1, Hungary*
[15]*ELTE, Eötvös Loránd University, H-1117 Budapest, Pázmány P. s. 1/A, Hungary*
[16]*Ewha Womans University, Seoul 120-750, Korea*
[17]*Florida A&M University, Tallahassee, Florida 32307, USA*
[18]*Florida State University, Tallahassee, Florida 32306, USA*
[19]*Georgia State University, Atlanta, Georgia 30303, USA*
[20]*Hanyang University, Seoul 133-792, Korea*
[21]*Hiroshima University, Kagamiyama, Higashi-Hiroshima 739-8526, Japan*
[22]*Department of Physics and Astronomy, Howard University, Washington, D.C. 20059, USA*
[23]*IHEP Protvino, State Research Center of Russian Federation, Institute for High Energy Physics, Protvino 142281, Russia*
[24]*University of Illinois at Urbana-Champaign, Urbana, Illinois 61801, USA*
[25]*Institute for Nuclear Research of the Russian Academy of Sciences, prospekt 60-letiya Oktyabrya 7a, Moscow 117312, Russia*
[26]*Institute of Physics, Academy of Sciences of the Czech Republic, Na Slovance 2, 182 21 Prague 8, Czech Republic*
[27]*Iowa State University, Ames, Iowa 50011, USA*
[28]*Advanced Science Research Center, Japan Atomic Energy Agency, 2-4 Shirakata Shirane, Tokai-mura,*
Naka-gun, Ibaraki-ken 319-1195, Japan
[29]*Jeonbuk National University, Jeonju, 54896, Korea*
[30]*Helsinki Institute of Physics and University of Jyväskylä, P.O.Box 35, FI-40014 Jyväskylä, Finland*
[31]*KEK, High Energy Accelerator Research Organization, Tsukuba, Ibaraki 305-0801, Japan*
[32]*Korea University, Seoul 02841, Korea*
[33]*National Research Center "Kurchatov Institute," Moscow 123098, Russia*
[34]*Kyoto University, Kyoto 606-8502, Japan*
[35]*Physics Department, Lahore University of Management Sciences, Lahore 54792, Pakistan*
[36]*Lawrence Livermore National Laboratory, Livermore, California 94550, USA*
[37]*Los Alamos National Laboratory, Los Alamos, New Mexico 87545, USA*
[38]*Department of Physics, Lund University, Box 118, SE-221 00 Lund, Sweden*
[39]*University of Maryland, College Park, Maryland 20742, USA*
[40]*Department of Physics, University of Massachusetts, Amherst, Massachusetts 01003-9337, USA*
[41]*MATE, Laboratory of Femtoscopy, Károly Róbert Campus, H-3200 Gyöngyös, Mátraiút 36, Hungary*
[42]*Department of Physics, University of Michigan, Ann Arbor, Michigan 48109-1040, USA*
[43]*Mississippi State University, Mississippi State, Mississippi 39762, USA*
[44]*Muhlenberg College, Allentown, Pennsylvania 18104-5586, USA*
[45]*Myongji University, Yongin, Kyonggido 449-728, Korea*
[46]*Nara Women's University, Kita-uoya Nishi-machi Nara 630-8506, Japan*
[47]*National Research Nuclear University, MEPhI, Moscow Engineering Physics Institute, Moscow 115409, Russia*
[48]*University of New Mexico, Albuquerque, New Mexico 87131, USA*
[49]*New Mexico State University, Las Cruces, New Mexico 88003, USA*
[50]*Physics and Astronomy Department, University of North Carolina at Greensboro, Greensboro, North Carolina 27412, USA*
[51]*Department of Physics and Astronomy, Ohio University, Athens, Ohio 45701, USA*
[52]*Oak Ridge National Laboratory, Oak Ridge, Tennessee 37831, USA*
[53]*IPN-Orsay, Univ. Paris-Sud, CNRS/IN2P3, Université Paris-Saclay, BP1, F-91406 Orsay, France*
[54]*PNPI, Petersburg Nuclear Physics Institute, Gatchina, Leningrad region 188300, Russia*
[55]*Pusan National University, Pusan 46241, Korea*
[56]*RIKEN Nishina Center for Accelerator-Based Science, Wako, Saitama 351-0198, Japan*

[57]*RIKEN BNL Research Center, Brookhaven National Laboratory, Upton, New York 11973-5000, USA*
[58]*Physics Department, Rikkyo University, 3-34-1 Nishi-Ikebukuro, Toshima, Tokyo 171-8501, Japan*
[59]*Saint Petersburg State Polytechnic University, St. Petersburg 195251 Russia*
[60]*Department of Physics and Astronomy, Seoul National University, Seoul 151-742, Korea*
[61]*Chemistry Department, Stony Brook University, SUNY, Stony Brook, New York 11794-3400, USA*
[62]*Department of Physics and Astronomy, Stony Brook University, SUNY, Stony Brook, New York 11794-3800, USA*
[63]*University of Tennessee, Knoxville, Tennessee 37996, USA*
[64]*Texas Southern University, Houston, Texas 77004, USA*
[65]*Department of Physics, Tokyo Institute of Technology, Oh-okayama, Meguro, Tokyo 152-8551, Japan*
[66]*Tomonaga Center for the History of the Universe, University of Tsukuba, Tsukuba, Ibaraki 305, Japan*
[67]*Vanderbilt University, Nashville, Tennessee 37235, USA*
[68]*Weizmann Institute, Rehovot 76100, Israel*
[69]*Institute for Particle and Nuclear Physics, Wigner Research Centre for Physics,*
Hungarian Academy of Sciences (Wigner RCP, RMKI) H-1525 Budapest 114, P.O. Box 49, Budapest, Hungary
[70]*Yonsei University, IPAP, Seoul 120-749, Korea*
[71]*Department of Physics, Faculty of Science, University of Zagreb, Bijenička c. 32 HR-10002 Zagreb, Croatia*
[72]*Department of Physics, School of Natural Sciences, University of Zambia, Great East Road Campus, Box 32379 Lusaka, Zambia*

(Received 17 February 2022; revised 4 November 2022; accepted 28 April 2023; published 21 June 2023)

We present measurements of the cross section and double-helicity asymmetry A_{LL} of direct-photon production in $\vec{p}+\vec{p}$ collisions at $\sqrt{s}=510$ GeV. The measurements have been performed at midrapidity ($|\eta|<0.25$) with the PHENIX detector at the Relativistic Heavy Ion Collider. At relativistic energies, direct photons are dominantly produced from the initial quark-gluon hard scattering and do not interact via the strong force at leading order. Therefore, at $\sqrt{s}=510$ GeV, where leading-order-effects dominate, these measurements provide clean and direct access to the gluon helicity in the polarized proton in the gluon-momentum-fraction range $0.02<x<0.08$, with direct sensitivity to the sign of the gluon contribution.

DOI: 10.1103/PhysRevLett.130.251901

In polarized-proton collisions, spin-asymmetry measurements are sensitive to the polarized partonic structure of the proton and allow the investigation of its spin decomposition. Determining how fundamental properties of a particle such as spin comprise its constituents is of great importance in understanding quantum chromodynamics (QCD). Perturbative QCD (pQCD) has been successful in describing unpolarized cross sections while spin-dependent observables have historically offered additional insights. Polarized deep-inelastic scattering (DIS) has shown that only part of the proton spin is carried by quarks. A large fraction of the proton spin was suggested to be carried by gluons [1–5]. DIS is sensitive to gluons only through high-order interactions and the polarized gluon distribution is significantly less constrained compared to the unpolarized gluon due to the (so far) limited kinematic coverage of polarized data. At the Relativistic Heavy Ion Collider collider (RHIC), gluons are accessible at leading order in the hard scattering. Measurements of the double-helicity asymmetry (A_{LL}) are directly sensitive to the polarized gluon distribution via longitudinally polarized $\vec{p}+\vec{p}$ collisions. Recent RHIC measurements of π^0 and jets at $\sqrt{s}=62.4$ and 200 GeV [6–10] that were included in global analyses have shown the first direct evidence of nonzero gluon-spin contributions to the spin of the proton [11,12] in the gluon momentum fraction (x) range larger than 0.05. Measurements at the higher energy of $\sqrt{s}=510$ GeV [13,14] have confirmed the nonzero gluon polarization and extended the minimum x reach to ≈0.01. Recent analysis by the Jefferson Lab Angular Momentum (JAM) Collaboration showed that the two scenarios of positive and negative gluon-spin contributions are indistinguishable from each other based on the existing data [15,16]. This can be resolved using direct-photon production in $\vec{p}+\vec{p}$ scattering, which is linearly sensitive to gluon helicity.

Direct photons are all those photons that are not coming from decays of final-state hadrons. The quark-gluon Compton process $qg\to q\gamma$ in proton-proton collisions at RHIC is the dominant contributor to the direct photons with transverse momentum larger than 5 GeV/c. Unlike hadrons and jets, direct photons do not involve color interactions in the final state. Therefore, they provide a direct probe to the initial state of colliding protons. The double-helicity asymmetry of direct-photon production in longitudinally polarized $\vec{p}+\vec{p}$ collisions is sensitive to both the sign and magnitude of the gluon-spin contributions

---

to the proton spin. For this reason, A_{LL} was thought to be a *golden* channel to access the gluon spin in the 1992 RHIC-spin proposal [17,18]. In this Letter, we report the first measurements of this observable.

The data were collected in 2013 with the PHENIX detector at RHIC [19] at $\sqrt{s} = 510$ GeV within pseudorapidity $|\eta| < 0.25$. We have extracted the inclusive and isolated direct-photon cross sections and A_{LL} of isolated photons. The primary detector for this measurement is an electromagnetic calorimeter (EMCal) [20] comprising two subsystems, a six-sector lead-scintillator (PbSc) detector, of which four are on the west arm and two on the east arm, and a two-sector lead glass (PbGl) detector on the east arm, each located 5 m radially from the beam line. Each sector covers a range of $|\eta| < 0.35$ and 22.5° in azimuth ϕ. The EMCal has fine granularity with each tower covering $\Delta\eta \times \Delta\phi \approx 0.011 \times 0.011$ (0.008×0.008) for PbSc (PbGl). Two photons from $\pi^0 \to \gamma\gamma$ decays are fully resolved up to a π^0 p_T of 12 (16) GeV/c in the PbSc (PbGl), and a shower profile analysis extends the γ/π^0 discrimination up to 30 GeV/c in these measurements. The energy calibration of each tower is obtained from the reconstructed π^0 mass.

The beam-beam counters (BBC) [21] cover $3.1 < |\eta| < 3.9$ and are located at ±144 cm from the interaction point along the beam line. The BBCs measure the longitudinal collision vertex and provide a minimum-bias trigger. The BBCs are also used as a luminosity ($\mathcal{L}$) monitor. Events with high-p_T photons are selected by an EMCal-based trigger requiring a minimum energy deposit of 3.7 GeV in an overlapping tile of 4×4 towers of the EMCal in coincidence with the minimum-bias trigger. The cross-section (A_{LL}) analysis uses an integrated luminosity of 11 (108) pb^{-1} with a z-vertex requirement of 10 (30) cm around the nominal interaction point. The photon-reconstruction and analysis method used here is similar to the previous PHENIX measurement at $\sqrt{s} = 200$ GeV [22,23]. Photons are identified by a shower-profile requirement that was calibrated using test-beam data, identified electrons, and decay photons from identified π^0. The method rejects ≈50% of hadrons depositing $E > 3$ GeV in the EMCal and accepts ≈98% of real photons. The time of flight (TOF) of particles is measured relative to the photon signal in the EMCal. A TOF requirement $|\mathrm{TOF}| < 10$ ns is used to reduce pileup events due to high collision rate (the average number of BBC triggered events per beam crossing varied in the range 0.04–0.17). A minimum-energy requirement $E_{\min} > 0.3$ GeV is applied for the EMCal clusters to reduce the background noise. The charged-particle veto of the photon sample is based on tracks in the drift chambers [24].

The experimental challenge in this measurement is the large photon background from hadron decays, primarily from $\pi^0 \to \gamma\gamma$ (≈80% of the decays) and $\eta \to \gamma\gamma$ (≈15%). Photon candidates that form a pair with another photon in the mass range $110 < M_{\gamma\gamma} < 160\ \mathrm{MeV/c^2}$ $(M_{\pi^0} \pm 3\sigma)$ with $E_\gamma > 300$ MeV are tagged as π^0 decay photons. A fiducial region for direct-photon candidates excludes 10 (12) towers (0.1 rad) from the edges of the PbSc (PbGl). Partner photons are accepted over the entire detector to improve the probability of observing both decay photons from the π^0. This method overestimates ≈8% more yield of photons from π^0 decays, $\gamma^{\rm inc}_{\pi^0}$, due to combinatorial background. A p_T -dependent correction is estimated from the fit of the background under the π^0 peak in the two-photon invariant-mass distribution. The inclusive direct-photon yield is then determined as

$$\gamma^{\rm inc}_{\rm dir} = \gamma^{\rm inc}_{\rm total} - (1 + R^{\rm miss}_{\pi^0} + \delta^{\gamma}_{h/\pi^0})\gamma^{\rm inc}_{\pi^0}, \qquad (1)$$

where we subtract the reconstructed inclusive photons from π^0 decay ($\gamma^{\rm inc}_{\pi^0}$), those missing their partner photons ($R^{\rm miss}_{\pi^0}\gamma^{\rm inc}_{\pi^0}$) and photons from other hadron decays ($\delta^{\gamma}_{h/\pi^0}\gamma^{\rm inc}_{\pi^0}$) from the total inclusive photon sample ($\gamma^{\rm inc}_{\rm total}$). If a partner photon of a π^0 decay is missed, it will not be reconstructed in the π^0 mass peak window. The ratio of π^0 decay photons that missed their partner photons to those that were reconstructed, $R^{\rm miss}_{\pi^0}$, is estimated using a single π^0 simulation with photon shower and detector geometry. The $\delta^{\gamma}_{h/\pi^0}$ is calculated by η, ω, η' over π^0 ratios based on the previous $\sqrt{s} = 200$ GeV measurement [25]: $\delta^{\gamma}_{h/\pi^0} \approx 0.28$, with $\delta^{\gamma}_{\eta/\pi^0} \approx 0.21$ and $\delta^{\gamma}_{\omega/\pi^0} \approx \delta^{\gamma}_{\eta'/\pi^0} \approx 0.035$. A PYTHIA [26] simulation showed that the variation of these ratios is less than 10% between 200 and 510 GeV within $6 < p_T < 30$ GeV/c. The difference is accounted for by assigning a systematic uncertainty.

In addition, we also measured the isolated direct-photon cross section with isolation criteria on the photon candidates, which can largely reduce the contributions from parton fragmentation and hadron decays. For any other particles within a cone of radius $r_{\rm cone} = \sqrt{(\delta\eta)^2 + (\delta\phi)^2} = 0.5$ of the signal photon, the sum of their energies is required to be less than 10% of the energy of the signal photon: $E_{\rm cone} < 0.1E_\gamma$. The energies of the neutral particles that pass charge-veto criteria were measured by the EMCal with a minimal threshold of 300 MeV. The momenta of the charged particles were measured by the drift chambers with a minimal threshold of 200 MeV/c. The efficiency of isolation criteria due to limited detector acceptance was corrected by using PYTHIA-simulated direct-photon events with the same isolation criteria as in the data. Similar to Eq. (1), the isolated direct-photon yield can be expressed as

$$\gamma^{\rm iso}_{\rm dir} = \gamma^{\rm iso}_{\rm total} - \gamma^{\rm iso}_{\pi^0} - (R^{\rm miss}_{\pi^0} + V\delta^{\gamma}_{h/\pi^0})\gamma^{\rm isopair}_{\pi^0}, \qquad (2)$$

where $\gamma^{\rm iso}_{\pi^0}$ is the π^0 tagged-photon yield when each of the π^0 decay photons passes the isolation requirement. $\gamma^{\rm isopair}_{\pi^0}$ is the yield when a photon from a π^0 decay passes the isolation requirement while its partner photon energy is not included in the isolation-cone energy sum. Therefore, $R^{\text{miss}}_{\pi^0}\gamma^{\text{isopair}}_{\pi^0}$ represents the yield of π^0 decay photons that are missing the energy of their partner photons. Similarly, the term $\delta^{\gamma}_{h/\pi^0}\gamma^{\text{isopair}}_{\pi^0}$ corrects for the photons from other hadron decays that pass the isolation requirement while the energy of the partner photon is not included in the isolation cone energy sum. To include the effect that one of the decay photons is vetoed by its partner decay photon due to isolation criteria, we use single η and detector simulations to calculate the ratio of η decay photons with and without isolation criteria, $V = \gamma^{\text{iso}}_{\eta}/\gamma^{\text{inc}}_{\eta}$, which varies from 0.01 to 0.1 depending on p_T.

The direct-photon cross section is calculated as

$$E\frac{d^3\sigma}{dp^3} = \frac{1}{\mathcal{L}} \cdot \frac{1}{2\pi p_T} \cdot \frac{1}{\Delta p_T \Delta y} \cdot \frac{r_{\text{pileup}} \cdot \gamma_{\text{dir}}}{\epsilon}, \qquad (3)$$

where ϵ includes corrections for the detector acceptance, photon reconstruction efficiency, trigger efficiency, and detector smearing effects and r_{pileup} is the correction for the pileup effects due to the large signal-integration time of the EMCal coupled with the high collision rate. It is approximately 0.8 (0.9) for inclusive (isolated) direct photons. The correction is obtained by a logarithmic extrapolation of the number of photons per event to zero event rate. The $\mathcal{L}$ is the integrated luminosity used for the analyzed data, and Δy is the rapidity range.

The main systematic uncertainty sources are from the global energy scale of tuning the π^0 mass-peak position and energy nonlinearity of the EMCal response at high p_T. These are calculated by a single π^0 or photon generator with a fast detector simulation and depending on p_T were determined to be 14%–19% (7%–13%) for the inclusive (isolated) direct-photon cross section. The systematic uncertainties due to π^0 yield extraction and relative fractions of other hadron decays over π^0 are 2%–12% (0.5%–2.5%) and 5%–14% (0.4%–6.0%) for the inclusive (isolated) direct-photon cross section. These contributions for the isolated direct-photon cross section are relatively small compared to the inclusive case as the isolation requirement largely reduces these backgrounds. The loss of photons from conversions in the material before the EMCal is estimated using a single-photon generator plus full GEANT detector simulation [27]. The material of the vertex tracker [28] leads to a $(12.8 \pm 1.9)\%$ probability for a photon to convert. This systematic uncertainty only contributes to the west arm, because in 2013 the east arm did not have a vertex-tracker installed. Conversions in other materials lead to photon losses of $(3 \pm 1)\%$ in the PbSc and $(4.5 \pm 1.3)\%$ in the PbGl. When calculating the direct-photon yield in Eq. (1) and Eq. (2), we vary the photon-conversion rate by its systematic uncertainty to get 1%–8% relative uncertainties of the direct-photon yield. The uncertainties from the EMCal detector resolution of 2%–8% and trigger of 2%–4.5% are also taken into account. Other uncertainties, including geometrical

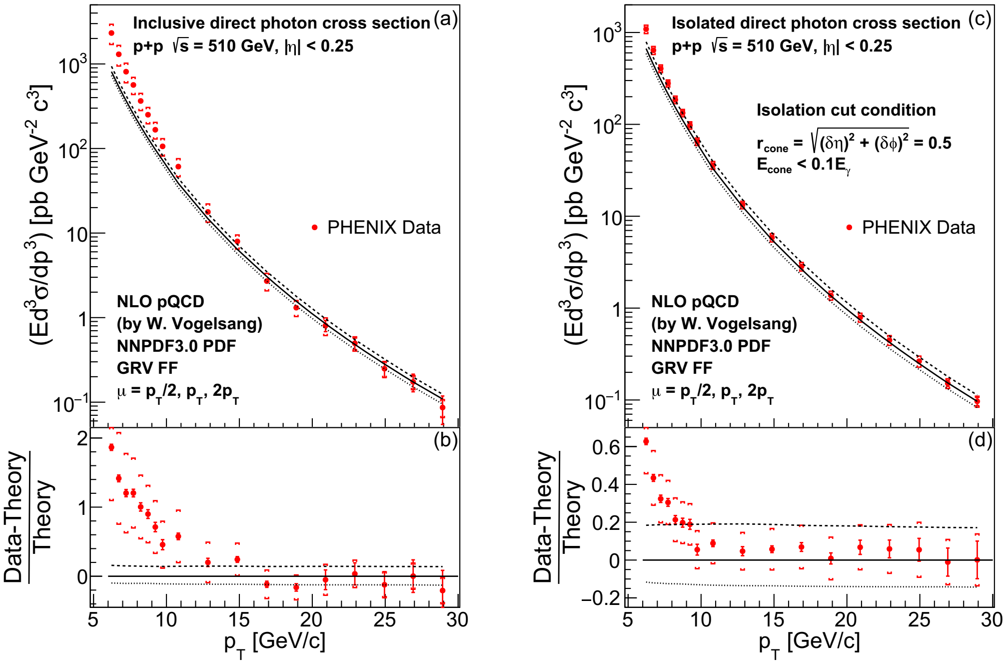

FIG. 1. Cross sections for (a) inclusive and (c) isolated direct photons as a function of p_T compared with next-to-leading-order (NLO) pQCD calculations [29,30] for different renormalization and factorization scales $\mu = p_T/2$ (dashed line), p_T (solid line), $2p_T$ (dotted line). The vertical bars show statistical uncertainties and square brackets are for systematic uncertainties. Not shown are 10% absolute luminosity uncertainties. Panels (b) and (d) show comparisons of data and calculations.

acceptance, trigger efficiencies, and pileup effect, are in total less than 7%.

Figure 1(a) shows the measured inclusive direct-photon cross section at midrapidity in $\vec{p}+\vec{p}$ collisions at $\sqrt{s} =$ 510 GeV compared with NLO pQCD calculations [29,30] using NNPDF3.0 parton-distribution functions (PDF) [31,32] and Glück-Reya-Vogt (GRV) fragmentation functions (FF) [33]. The pseudorapidity range for this measurement is $|\eta| < 0.25$ after the fiducial requirement that removes edge towers of the EMCal. The calculation is in good agreement with the data within the uncertainties for $p_T > 12$ GeV$/c$, but underestimates the yield by up to a factor of ≈ 3 for $p_T < 12$ GeV$/c$. This discrepancy is possibly due to multiparton interactions and parton showers [34–38]. The isolated direct-photon cross section is shown in Fig. 1(c) as a function of p_T and compared with the NLO pQCD calculation [29,30] using NNPDF3.0 [31,32] and GRV FF [33]. The calculation is in good agreement with the data within the uncertainties, with slight overestimation in the lowest p_T bins.

The double-helicity asymmetry is defined as

$$A_{LL} = \frac{\Delta\sigma}{\sigma} = \frac{\sigma_{++} - \sigma_{+-}}{\sigma_{++} + \sigma_{+-}}, \qquad (4)$$

where σ_{++} (σ_{+-}) is the cross section for the same (opposite) helicity proton-proton collisions. This can be rewritten in terms of particle yield and beam polarizations:

$$A_{LL} = \frac{1}{P_B P_Y} \frac{N_{++} - RN_{+-}}{N_{++} + RN_{+-}}, \qquad (5)$$

where N_{++} (N_{+-}) is the number of isolated direct photons from the collisions with the same (opposite) helicities. P_B (P_Y) are the polarizations for the blue (yellow) proton beams, and the average values in 2013 were 0.55 (0.57) [39]. $R = (\mathcal{L}_{++}/\mathcal{L}_{+-})$ is the relative luminosity that is measured by the BBC. The systematic contribution of R to A_{LL} was found to be 3.8×10^{-4} [13].

The asymmetry was calculated for photon candidates that passed the same time-of-flight, minimum-energy, and isolation requirements as in the cross-section analysis. A z-vertex requirement of 30 cm is used for the asymmetry measurement. The asymmetry contribution for background photons from π^0 's decay was calculated from the sideband regions (47–97 and 177–227 MeV$/c^2$) below and above the π^0 mass peak (112–162 MeV$/c^2$) using the inclusive photon sample due to the limited statistics in the isolated photon sample. The asymmetry for other hadron decays (mostly η decays) was taken as A_{LL}^{η} from previous PHENIX measurements at $\sqrt{s} = 200$ GeV [6] by assuming x_T scaling. The difference in A_{LL}^{η} between 200 and 510 GeV for a given x_T is expected to be much smaller than the experimental uncertainty of the 200 GeV result which was used to assign a systematic uncertainty [11,12]. The background-corrected asymmetry can be calculated as

$$A_{LL}^{\mathrm{dir}} = \frac{A_{LL}^{\mathrm{total}} - r_{\pi^0} A_{LL}^{\pi^0} - r_h A_{LL}^{\eta}}{1 - r_{\pi^0} - r_h}, \qquad (6)$$

where r_{π^0} (10%–14%) and r_h (0.6%–1.4%) are background fractions of π^0 and other hadron-decay photons, respectively. We used a bunch-shuffling technique which assigned a random spin polarization to each bunch and examined the distribution of resulting asymmetries ensure there were no false asymmetries arising from unknown systematic effects [6]. The data were divided into subgroups according to the bunch spin patterns that were used to fill the RHIC rings, and calculated asymmetries were found to be consistent.

Figure 2 shows the double-helicity asymmetry of isolated direct-photon production in longitudinally polarized proton-proton collisions at $\sqrt{s} = 510$ GeV for $6 < p_T <$ 20 GeV$/c$. The corresponding gluon momentum fraction is $x \approx 2p_T/\sqrt{s}$. In the asymmetry measurement, systematic effects are largely canceled. The systematic uncertainties in Fig. 2 include point-to-point uncertainties from background estimation and false asymmetries in the background due to pileup effects at low p_T. The NLO pQCD calculation

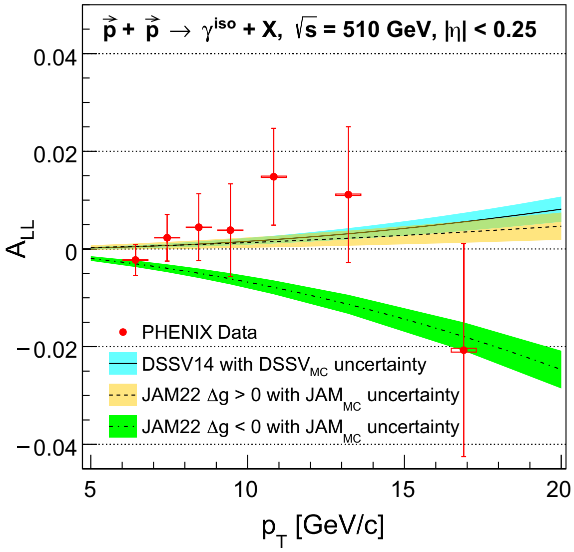

FIG. 2. Double-helicity asymmetry A_{LL} vs p_T for isolated direct-photon production in polarized $p+p$ collisions at $\sqrt{s} =$ 510 GeV at midrapidity. Vertical error bars (boxes) represent the statistical (systematic) uncertainties. The systematic uncertainties for $p_T < 10$ GeV/c are smaller than the marker size. Not shown are a 3.9×10^{-4} shift uncertainty from relative luminosity and a 6.6% scale uncertainty from polarization. The DSSV14 and JAM22 calculations are shown with 1σ uncertainty bands obtained from MC replicas [11,15,16,40,41]. JAM22 calculations are based on PDF sets from the global analysis of the JAM Collaboration [16], and the code to calculate the asymmetries was provided by W. Vogelsang.

was obtained using the DSSV14 polarized PDFs, the NNPDF3.0 unpolarized PDFs and the GRV FF for the renormalization and factorization scales $\mu = p_T$ with the 1σ uncertainty band determined via MC replicas (a sampling variant of the DSSV14 set of helicity parton densities) [11,40,41]. The calculation is in good agreement with the results, within experimental uncertainties.

The two dashed curves in Fig. 2 come from the global analysis of the JAM Collaboration [15,16]. They found there are two distinct sets of solutions for the polarized gluon PDF, Δg, which differ in sign. Even though the solutions with $\Delta g < 0$ violate the positivity assumption, $|\Delta g| < g$, all previous data cannot exclude those solutions due to the mixed contributions from quark-gluon and gluon-gluon interactions. However, the direct-photon A_{LL} comes mainly from the quark-gluon interactions and has $\chi^2 = 4.7$ and 12.6 for 7 data points for the $\Delta g > 0$ and $\Delta g < 0$ solutions, respectively, with the difference of 7.9 between χ^2 values implying that the negative solution is disfavored at more than the 2.8σ level.

In summary, PHENIX has measured the cross section and A_{LL} of direct photons at midrapidity in $\vec{p} + \vec{p}$ collisions at $\sqrt{s} = 510$ GeV. The NLO pQCD calculations are consistent with the results except at lower p_T where the calculations underestimate the inclusive direct-photon cross section. With isolation criteria, the partonic level calculation is in better agreement with the measurement. This is the first measurement of the A_{LL} of direct photons, which is sensitive to the polarized-gluon distribution inside the proton. Our data are well consistent with the positive gluon-spin contributions and strongly disfavor the negative gluon-spin scenario, that the previously published data were unable to resolve.

We thank the staff of the Collider-Accelerator and Physics Departments at Brookhaven National Laboratory and the staff of the other PHENIX participating institutions for their vital contributions. We also thank W. Vogelsang for providing the code for direct photon asymmetry calculations. We acknowledge support from the Office of Nuclear Physics in the Office of Science of the Department of Energy, the National Science Foundation, Abilene Christian University Research Council, Research Foundation of SUNY, and Dean of the College of Arts and Sciences, Vanderbilt University (U.S.A), Ministry of Education, Culture, Sports, Science, and Technology and the Japan Society for the Promotion of Science (Japan), Natural Science Foundation of China (People's Republic of China), Croatian Science Foundation and Ministry of Science and Education (Croatia), Ministry of Education, Youth and Sports (Czech Republic), Centre National de la Recherche Scientifique, Commissariat à l'Énergie Atomique, and Institut National de Physique Nucléaire et de Physique des Particules (France), J. Bolyai Research Scholarship, EFOP, the New National Excellence Program (ÚNKP), NKFIH, and OTKA (Hungary), Department of Atomic Energy and Department of Science and Technology (India), Israel Science Foundation (Israel), Basic Science Research and SRC(CENuM) Programs through NRF funded by the Ministry of Education and the Ministry of Science and ICT (Korea), Physics Department, Lahore University of Management Sciences (Pakistan), Ministry of Education and Science, Russian Academy of Sciences, Federal Agency of Atomic Energy (Russia), VR and Wallenberg Foundation (Sweden), University of Zambia, the Government of the Republic of Zambia (Zambia), the U.S. Civilian Research and Development Foundation for the Independent States of the Former Soviet Union, the Hungarian American Enterprise Scholarship Fund, the US-Hungarian Fulbright Foundation, and the US-Israel Binational Science Foundation.

---

[*] Deceased.

[†] PHENIX Spokesperson.
akiba@rcf.rhic.bnl.gov

[1] J. Ashman *et al.* (European Muon Collaboration), A measurement of the spin asymmetry and determination of the structure function g1 in deep inelastic muon-proton scattering, Phys. Lett. B **206**, 364 (1988).

[2] J. Ashman *et al.* (European Muon Collaboration), An investigation of the spin structure of the proton in deep inelastic scattering of polarised muons on polarised protons, Nucl. Phys. **B328**, 1 (1989).

[3] B. Adeva *et al.* (Spin Muon Collaboration), Spin asymmetries A_1 and structure functions g_1 of the proton and the deuteron from polarized high energy muon scattering, Phys. Rev. D **58**, 112001 (1998).

[4] V. Y. Alexakhin *et al.* (COMPASS Collaboration), The deuteron spin-dependent structure function g1d and its first moment, Phys. Lett. B **647**, 8 (2007).

[5] A. Airapetian *et al.* (HERMES Collaboration), Precise determination of the spin structure function g_1 of the proton, deuteron, and neutron, Phys. Rev. D **75**, 012007 (2007).

[6] A. Adare *et al.* (PHENIX Collaboration), Inclusive double-helicity asymmetries in neutral-pion and eta-meson production in $\vec{p} + \vec{p}$ collisions at $\sqrt{s} = 200$ GeV, Phys. Rev. D **90**, 012007 (2014).

[7] A. Adare *et al.* (PHENIX Collaboration), Gluon-Spin Contribution to the Proton Spin from the Double-Helicity Asymmetry in Inclusive π^0 Production in Polarized $p + p$ Collisions at $\sqrt{s} = 200$ GeV, Phys. Rev. Lett. **103**, 012003 (2009).

[8] A. Adare *et al.* (PHENIX Collaboration), Inclusive cross section and double helicity asymmetry for π^0 production in $p + p$ collisions at $\sqrt{s} = 62.4$ GeV, Phys. Rev. D **79**, 012003 (2009).

[9] B. I. Abelev *et al.* (STAR Collaboration), Longitudinal and transverse spin asymmetries for inclusive jet production at midrapidity in polarized $p + p$ collisions at $\sqrt{s}$=200 GeV, Phys. Rev. D **86**, 032006 (2012).

[10] L. Adamczyk *et al.* (STAR Collaboration), Precision Measurement of the Longitudinal Double-Spin Asymmetry for

Inclusive Jet Production in Polarized Proton Collisions at $\sqrt{s} = 200$ GeV, Phys. Rev. Lett. **115**, 092002 (2015).

[11] D. de Florian, R. Sassot, M. Stratmann, and W. Vogelsang, Evidence for Polarization of Gluons in the Proton, Phys. Rev. Lett. **113**, 012001 (2014).

[12] E. N. Nocera, R. D. Ball, S. Forte, G. Ridolfi, and J. Rojo (NNPDF Collaboration), A first unbiased global determination of polarized PDFs and their uncertainties, Nucl. Phys. **B887**, 276 (2014).

[13] A. Adare *et al.* (PHENIX Collaboration), Inclusive cross section and double-helicity asymmetry for π^0 production at midrapidity in $p + p$ collisions at $\sqrt{s} = 510$ GeV, Phys. Rev. D **93**, 011501 (2016).

[14] J. Adam *et al.* (STAR Collaboration), Longitudinal double-spin asymmetry for inclusive jet and dijet production in $p + p$ collisions at $\sqrt{s} = 510$ GeV, Phys. Rev. D **100**, 052005 (2019).

[15] Y. Zhou, N. Sato, and W. Melnitchouk (JAM Collaboration), How well do we know the gluon polarization in the proton?, Phys. Rev. D **105**, 074022 (2022).

[16] C. Cocuzza, W. Melnitchouk, A. Metz, and N. Sato (JAM Collaboration), Polarized antimatter in the proton from a global QCD analysis, Phys. Rev. D **106**, L031502 (2022).

[17] G. Bunce, A. Carroll, E. Courant, R. Fernow, Y. Lee, D. Lowenstein, Y. Makdisi, L. Ratner, T. Roser, and M. Tannenbaum, Proposal on spin physics using the RHIC polarized collider, Report No. BNL-104822-2014-IR, 1992, 10.2172/1151313.

[18] G. Bunce, N. Saito, J. Soffer, and W. Vogelsang, Prospects for spin physics at RHIC, Annu. Rev. Nucl. Part. Sci. **50**, 525 (2000).

[19] K. Adcox *et al.* (PHENIX Collaboration), PHENIX detector overview, Nucl. Instrum. Methods Phys. Res., Sect. A **499**, 469 (2003).

[20] L. Aphecetche *et al.* (PHENIX Collaboration), PHENIX calorimeter, Nucl. Instrum. Methods Phys. Res., Sect. A **499**, 521 (2003).

[21] M. Allen *et al.* (PHENIX Collaboration), PHENIX inner detectors, Nucl. Instrum. Methods Phys. Res., Sect. A **499**, 549 (2003).

[22] S. S. Adler *et al.* (PHENIX Collaboration), Measurement of Direct Photon Production in $p + p$ Collisions at $\sqrt{s} = 200$ GeV, Phys. Rev. Lett. **98**, 012002 (2007).

[23] A. Adare *et al.* (PHENIX Collaboration), Direct photon production in $p + p$ collisions at $\sqrt{s} = 200$ GeV at midrapidity, Phys. Rev. D **86**, 072008 (2012).

[24] K. Adcox *et al.* (PHENIX Collaboration), PHENIX central arm tracking detectors, Nucl. Instrum. Methods Phys. Res., Sect. A **499**, 489 (2003).

[25] A. Adare *et al.* (PHENIX Collaboration), Measurement of neutral mesons in $p + p$ collisions at $\sqrt{s} = 200$ GeV and scaling properties of hadron production, Phys. Rev. D **83**, 052004 (2011).

[26] T. Sjostrand, S. Mrenna, and P. Z. Skands, PYTHIA 6.4 physics and manual, J. High Energy Phys. 05 (2006), 026.

[27] R. Brun, F. Bruyant, F. Carminati, S. Giani, M. Maire, A. McPherson, G. Patrick, and L. Urban, GEANT detector description and simulation tool, Reports No. CERN-W5013, No. CERN-W-5013, No. W5013, No. W-5013, 1994, 10.17181/CERN.MUHF.DMJ1.

[28] W. Sondheim, Mechanics and assembly of the silicon vertex detector for the PHENIX experiment at RHIC, Phys. Procedia **37**, 993 (2012).

[29] L. E. Gordon and W. Vogelsang, Polarized and unpolarized prompt photon production beyond the leading order, Phys. Rev. D **48**, 3136 (1993).

[30] L. E. Gordon and W. Vogelsang, Polarized and unpolarized isolated prompt photon production beyond the leading order, Phys. Rev. D **50**, 1901 (1994).

[31] R. D. Ball, V. Bertone, S. Carrazza, C. S. Deans, L. Del Debbio, S. Forte, A. Guffanti, N. P. Hartland, J. I. Latorre, J. Rojo, and M. Ubiali, Parton distributions for the LHC run II, J. High Energy Phys. 04 (2015) 040.

[32] M. Bonvini, S. Marzani, J. Rojo, L. Rottoli, M. Ubiali, R. D. Ball, V. Bertone, S. Carrazza, and N. P. Hartland, Parton distributions with threshold resummation, J. High Energy Phys. 09 (2015) 191.

[33] M. Glück, E. Reya, and A. Vogt, Parton structure of the photon beyond the leading order, Phys. Rev. D **45**, 3986 (1992).

[34] P. Nason, A new method for combining NLO QCD with shower Monte Carlo algorithms, J. High Energy Phys. 11 (2004) 040.

[35] S. Frixione, P. Nason, and C. Oleari, Matching NLO QCD computations with parton-shower simulations: The POWHEG method, J. High Energy Phys. 11 (2007) 070.

[36] S. Alioli, P. Nason, C. Oleari, and E. Re, A general framework for implementing NLO calculations in shower Monte Carlo programs: The POWHEG BOX, J. High Energy Phys. 06 (2010) 043.

[37] T. Ježo, M. Klasen, and F. König, Prompt photon production and photon-hadron jet correlations with POWHEG, J. High Energy Phys. 11 (2016) 033.

[38] M. Klasen, C. Klein-Bösing, and H. Poppenborg, Prompt photon production and photon-jet correlations at the LHC, J. High Energy Phys. 03 (2018) 081.

[39] A. A. Poblaguev, A. Zelenski, G. Atoian, Y. Makdisi, and J. Ritter, Systematic error analysis in the absolute hydrogen gas jet polarimeter at RHIC, Nucl. Instrum. Methods Phys. Res., Sect. A **976**, 164261 (2020).

[40] D. de Florian, R. Sassot, M. Stratmann, and W. Vogelsang, Global Analysis of Helicity Parton Densities and their Uncertainties, Phys. Rev. Lett. **101**, 072001 (2008).

[41] D. de Florian, G. A. Lucero, R. Sassot, M. Stratmann, and W. Vogelsang, Monte Carlo sampling variant of the DSSV14 set of helicity parton densities, Phys. Rev. D **100**, 114027 (2019).